Birefringence and Orientation Parameters of Cold-Drawn Viscose Fibers

I. M. Fouda, E. A. Seisa

Physics Department, Faculty of Science, Mansoura University, Mansoura, Egypt

Received 9 March 2007; accepted 15 May 2007
DOI 10.1002/app.26849
Published online 17 July 2007 in Wiley InterScience (www.interscience.wiley.com).

ABSTRACT: This study was carried out by two beam polarizing interference Pluta microscope to obtain changes undrawn viscose fibers. Application of the appropriate mathematical equations indicates that the refractive indices in the direction of the drawing force increase with increasing the draw ratio and decrease in the perpendicular direction. The changes in the draw ratio were evaluated to obtain the shrinkage stress, the mechanical function factors $\langle P_2(\cos\theta)\rangle$ and $\langle P_4(\cos\theta)\rangle$, the average work per chain W' for a collection of chains, and the average mechanical orientation. The optical results were to obtain the three optical orientation functions, the dielectric constant and the dielectric susceptibility and the average orientation function. Also calculation of the intrinsic crystalline Δn_c^o and amorphous Δn_a^o birefringence. Evaluation of another opto-mechanical parameters were given, too. An empirical formula was suggested to evaluate the relationship between the draw ratio and some determined opto mechanical parameters. Illustrations using microinterferogram, graphs, and tables are given. © 2007 Wiley Periodicals, Inc. J Appl Polym Sci 106: 1768–1776, 2007

Key words: interferometry; orientation; dielectric; crystalline and amorphous intrinsic birefringence; viscose fibres

INTRODUCTION

The study of optical anisotropy in viscose fibers plays an important role in the knowledge of the molecular arrangement within these fibers. Double refraction depends on the molecular orientation in viscose fibers as it contains contributions from the polarizabilities of all molecular units in the sample.[1]

Intensive interferometric investigations have been carried out by many authors to study, improve, and develop various characteristics for investigations in fibrous materials.[2–6]

A several number of investigations have been devoted to the physical properties of viscose fibers, including mechanical ones such as elastic modules, yield strength, elastic shear modules, and compressibility, which indicate how particular materials react when stressed. There properties can be employed to seek an explanation of the observed macroscopic behavior of the material in molecular term, which include details of the chemical composition and physical structure. Optical anisotropy produced in fibers gives valuable information for characterization of these fibers on the molecular level and various processes have been used and developed for this purpose. Optical anisotropy changes the random molecular orientation of the isotropic polymers. All measurements were confined to room temperature and the elastic constants were obtained as a function of molecular orientation as determined by the draw ratio and birefringence.[7]

The present article used double refraction polarized interference Pluta microscope in conjunction with a micro-strain device to study the opto-mechanical properties. These device were used to measure stress as well strain and used to measure both the refractive indices for the two directions parallel and perpendicular. The optical and mechanical data were used to give the orientation functions, the crystalline and amorphous intrinsic birefringence, dielectric constant, dielectric susceptibility, surface reflectivity, and other opto-mechanical parameters.

THEORETICAL CONSIDERATIONS

The two beam interference techniques in conjunction with a mechanical device were used for determining principle optical parameters. These parameters with their relations to the mechanical parameters were given recently extensively elsewhere.[2,6,8]

Mechanical parameters

The shrinkage ratio increases with increasing draw ratio in good agreement with the expected relationship[9]

$$\delta_r = 1 - 1/D \tag{1}$$

where D is the draw ratio (final fiber length/starting length). If the shrinkage force could be measured,

Correspondence to: E. A. Seisa (seisa@mans.edu.eg).

Journal of Applied Polymer Science, Vol. 106, 1768–1776 (2007)

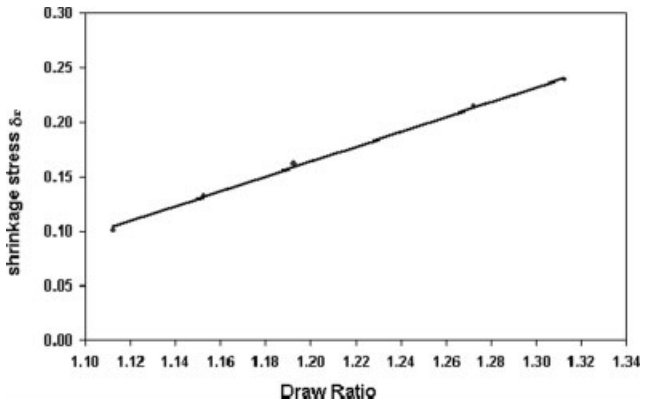

Figure 1 Variations of the shrinkage stress by changing the draw ratio of viscose fibers.

the stress optical coefficient can be used to calculate the number of monomer units per link. The relation (1) was shown in Figure 1.

On the aggregate model the low strain mechanical anisotropy is related to the orientation functions $\langle P_2(\theta)\rangle$ and $\langle P_4(\theta)\rangle$. These functions provide some understanding of the mechanism of deformation. By considering the network as of freely jointed chains of identical links called random links, $\langle P_2(\cos\ \theta)\rangle$ was given by[10,11]

$$\langle P_2(\theta)\rangle = \frac{1}{2}\left[\frac{2+U^2}{1-U^2} - \frac{3U\cos^{-1}U}{(1-U^2)^{3/2}}\right] \tag{2}$$

where $U = D^{-3/2}$. Using the Treloar[12] expression for the inverse Langevin function to obtain $\langle P_4(\theta)\rangle$

$$\langle P_4(\theta)\rangle = \frac{1}{8}\left\{\frac{35}{(1-U^2)^2}\left[1+\frac{U^2}{2}-\frac{3U\cos^{-1}U}{2(1-U^2)^{1/2}}\right] - \frac{30}{1-U^2}\left[1-\frac{U\cos^{-1}U}{(1-U^2)^{1/2}}\right]+3\right\}. \tag{3}$$

Figure 2 shows the mechanical factors $\langle P_2(\theta)\rangle$ and $\langle P_4(\theta)\rangle$ as a function of the draw ratio.

Orientation function

For optically anisotropic fibers the refractive index and the double refraction are parameters that characterize the structure of the material. The double refraction of fibers arises from the orientation of the polymer molecules along the fiber axis, averaged over the crystalline and noncrystalline regions of the fibers. This molecular orientation influences not only the mechanical properties, but also other physical properties of the yarn. Besides the various techniques (i.e. IR, UV, NMR, and ESR) refractive index and birefringence measurements still constitute a valuable method for the characterization of fibers.

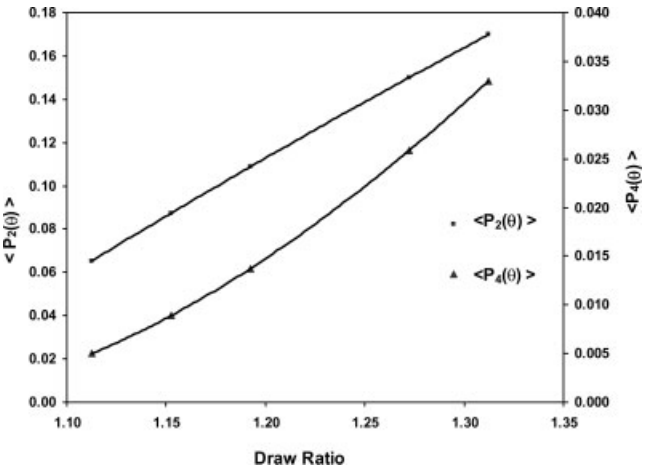

Figure 2 Mechanical orientation factors $\langle P_2(\theta)\rangle$ and $\langle P_4(\theta)\rangle$ as a function of the draw ratio.

The optical orientation function $f_\Delta(\theta)$ was calculated by Hermans[11] and Ward[13,14] from the following

$$f_\Delta(\theta) = \Delta n/(\Delta n)_{\max} \tag{4}$$

where $(\Delta n)_{\max}$ is the maximum birefringence of a fully oriented fiber. Its value has been previously[11] determined to be (0.055) for viscose fiber. Figure 3 shows the relation between the average Harman s orientation function with different draw ratios at room temperature.

Hermans represented the orientation function $f(\theta)$ by a series of spherical harmonics[11,15,16] (Fourier series) as follows:

$$f(\theta) = \sum_{n=0}^{\infty}\left(n+\frac{1}{2}\right)\langle f_n\rangle f_n(\theta) \tag{5}$$

where the odd components are all zero and the first three even components were given by $f_2(\theta)$, $f_4(\theta)$,

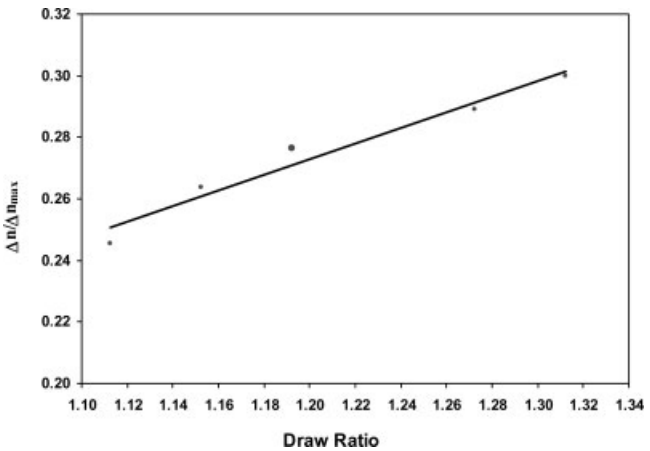

Figure 3 The relationship between the average Harman s orientation function at different draw ratios.

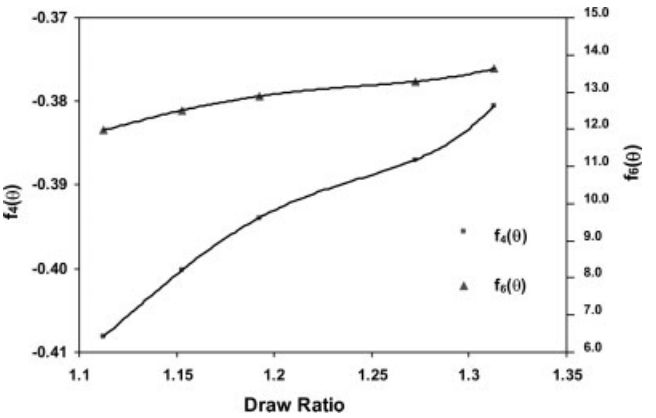

Figure 4 The relationship between the optical orientation functions $f_4(\theta)$ and $f_6(\theta)$ and draw ratio of viscose fibers at room temperature.

and $f_6(\theta)$. Figure 4 shows the relationship between the optical orientation functions $f_4(\theta)$ and $f_6(\theta)$ with different draw ratios of viscose fibers at room temperature. A sample with orientation function, may be considered to consist of perfectly aligned molecules of the mass fraction f and randomly oriented molecules of the mass fraction $(1 - f)$.

The deformations of a semi-crystalline polymer can be described by the kratky model.[3,17] On the basis of this model, Zbinden has derived an expression for the distribution of function with the draw ratios.[18] From this expression the orientation function can be calculated and the result was

$$f = 1 - \frac{3}{2}\left[1 - \frac{D^3}{D^3 - 1} + \frac{D^3}{(D^3 - 1)^{3/2}}\cos^{-1}\left(\frac{1}{D^{3/2}}\right)\right] \quad (6)$$

This relation show the dependence of the mechanical orientation functions on the draw ratio as shown in Figure 5.

Using the estimated value of the crystallinity we can then calculate the value of the orientation function of the amorphous phase according to the following equation,

$$f_a = \frac{f_{\text{tot}} - \chi_c f_c}{(1 - \chi_c)} \quad (7)$$

where f_{tot} is the total orientation function, which calculated as discussed elsewhere,[19] f_a and f_c are the orientation functions of the amorphous and crystalline regions respectively.

The orientation of the crystalline phase has been calculated from Gaylord's theoretical analysis[20] of stress induced crystallization in Gaussian networks whose results have been shown to be in good agreement with various experimental data.[21,22] These analysis results in the following expression for f_c as a function of draw ratio

$$f_c = \frac{1}{2}\left(\frac{3D^3}{2 + D^3} - 1\right) \quad (8)$$

Relation between dielectric constant and dielectric susceptibility

The complex electric inductive capacity is closely connected with the optical properties, as the refractive index and the absorption index. The relationships is given by

$$\varepsilon = \frac{1 + 2(n^2 - 1/n^2 + 2)}{1 - (n^2 - 1/n^2 + 2)} \quad (9)$$

$$\eta = \frac{\varepsilon - 1}{4\pi} \quad (10)$$

So the dielectric constant and dielectric susceptibility play an important role with the dielectric polarizability and dynamic-mechanical parameters as discussed elsewhere.[23]

Calculation of the surface reflectivity

The surface reflectivity of a polymer for light at normal incidence can be estimated from Fresnel equation[24] and a knowledge of $\overline{n}$. Thus the percentage reflection $\overline{R}$ (in air) is given by

$$\overline{R} = \left(\frac{\overline{n} - 1}{\overline{n} + 1}\right)^2 \times 100 \quad (11)$$

where $\overline{n}$ is the mean refractive index. Values of actual draw ratio, dielectric constant $\varepsilon^{\parallel}$, $\varepsilon^{\perp}$, $\overline{\varepsilon}$ the dielectric susceptibility $\eta^{\parallel}$, $\eta^{\perp}$, $\overline{\eta}$ and the surface reflectivity $\overline{R}$ as shown in Table I.

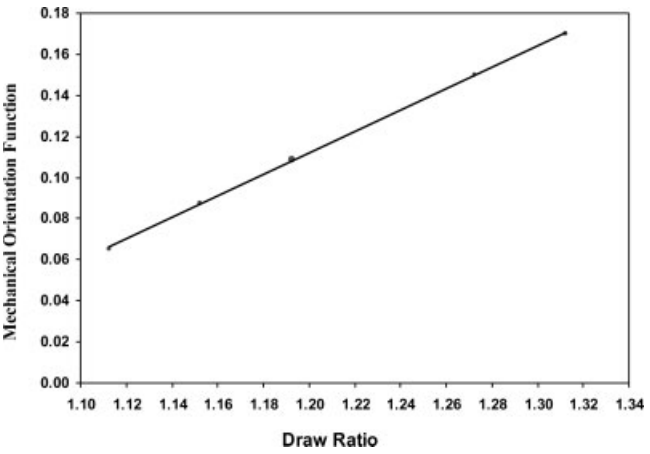

Figure 5 Shows the dependence of the mechanical orientation functions on the draw ratio.

TABLE I
Values of Actual Draw Ratio, Dielectric Constant $\varepsilon^{\parallel}$, $\varepsilon^{\perp}$, $\bar{\varepsilon}$, the Dielectric Susceptibility $\eta^{\parallel}$, $\eta^{\perp}$, $\bar{\eta}$ and the Surface Reflectivity $\overline{R}$

D.R	$\varepsilon^{\parallel}$	$\varepsilon^{\perp}$	$\bar{\varepsilon}$	$\eta^{\parallel}$	$\eta^{\perp}$	η	$\overline{R}$
1.113	2.345	2.304	2.325	0.10707	0.1038	0.10543	2.2164
1.153	2.347	2.303	2.325	0.10719	0.1037	0.10543	2.2164
1.192	2.348	2.302	2.325	0.10727	0.1036	0.10542	2.2160
1.273	2.349	2.301	2.325	0.10736	0.1035	0.10543	2.2164
1.313	2.350	2.300	2.325	0.10746	0.1035	0.10545	2.2171

Plate 1 Shows photographs of the totally duplicated image for viscose fibers.

Birefringence–strain relationship

As from the well known Mooney-Rivilin equation, the birefringence-strain relation is given as follows[25]

$$\Delta n = (D - D^{-2})\left(A_1 + \frac{A_2}{D}\right) \tag{12}$$

A plot of $\Delta n/(D - D^{-2})$ against the reciprocal elongation D^{-1} gives straight line whose slope A_2 and intercept with the ordinate A_1. The values obtained for A_1 and A_2 are -0.0971 and 0.1551, respectively, were determined from Figure 6. In general, the ratio A_2/A_1 is approximately similar to C_2/C_1 for the Mooney-Rivilin equation, as the birefringence known remains proportional to the stress.

EXPERIMENTAL RESULTS AND DISCUSSION

A Pluta polarizing interference microscope in conjunction with a micro-strain device, described elsewhere[26,27] were used to study the optical mechanical and structural properties of viscose fibers. This fiber fixed on a glass slide in a suitable position in the drawing device. A glass cover was placed on this fiber that was immersed in a liquid of refractive index $n_L = 1.528$ at 21.5°C using monochromatic light of wavelength 546 nm. The device was transferred to the Pluta microscope, which was adjusted in the totally duplicated image of viscose fibers, where the two fringe shifts for light vibrating parallel and perpendicular to the fiber axis were shown. Plate 1 shows selected photographs of the obtained to totally duplicated image for drawn viscose fibers. P1

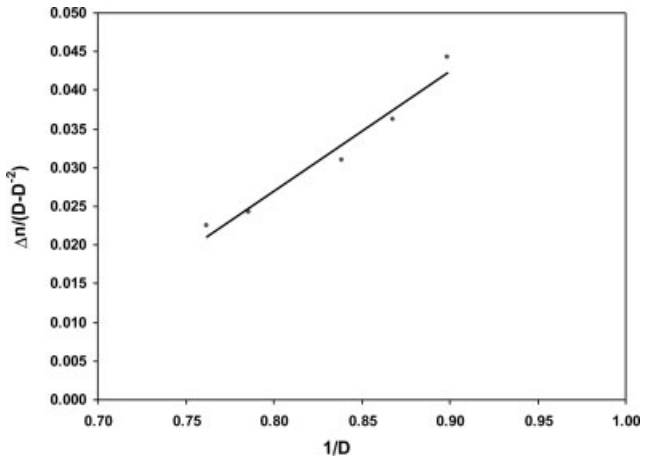

Figure 6 The relationship between $\Delta n/(D - D^{-2})$ against the reciprocal elongation D^{-1}.

Measurement of transverse sectional area

The cross section of the viscose fibers has been seen by high power optical microscope shows irregular shape. The cross sectional area A is found to be 1.165×10^{-3} mm^2.

The initial value of unknown draw ratio for any fiber

To estimate the initial draw ratio of any fiber sample, the refractive indices and the birefringence determined by using the opto-mechanical system which was designed and discussed in detail previously.[8] So by plotting the birefringence as, a function of the draw ratio leads to found the actual draw ratio as shown by Figure 7, the actual draw ratio was found to be $(D + 0.113)$.

Crystallinity measurements

The crystallinity can be measured by a different number of methods which have different techniques, i.e. IR, DSC, specific enthalpy, X-ray scattering intensity, nuclear magnetic resonance, etc. But to explain our present work it was found that the present described method was the available technique in our laboratory, for the effect of structures transformation due to cold drawing.

As well known n_{iso} is linearly proportional to the density and the density shows a linear dependence on the crystallinity χ_c, we can write crystallinity for

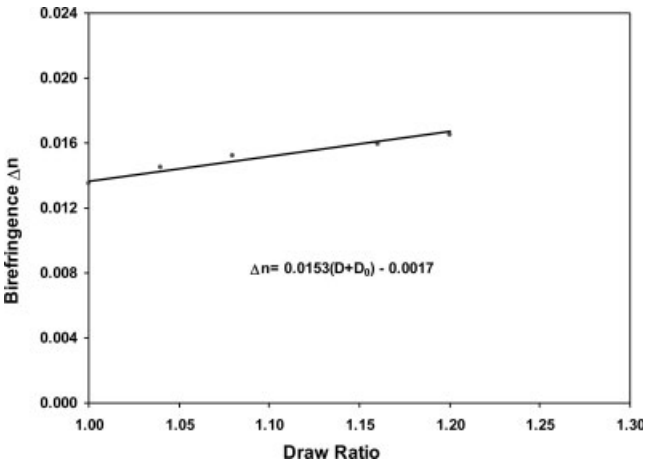

Figure 7 Determination of the actual draw ratio of viscose fibers.

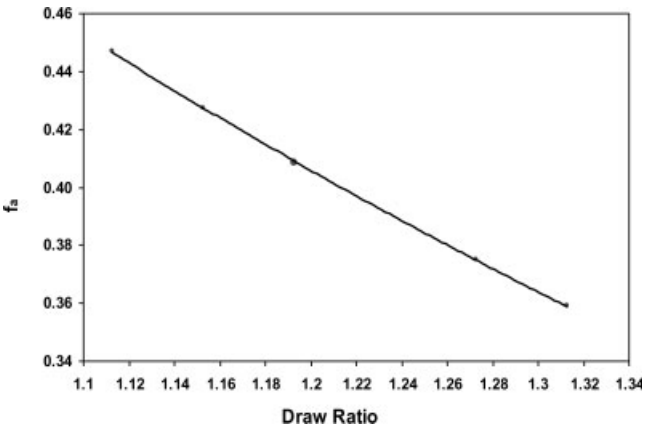

Figure 9 Relationship between the amorphous orientation function f_a and draw ratio for viscose fibers.

the regenerated celluloses as the following equation[28]

$$\chi_c = \frac{n_{\text{iso}} - 1.5077}{0.0456} \tag{13}$$

where n_{iso} amorphous = 1.5077 and n_{iso} crystalline = 1.5533. This equation allows us to evaluate χ_c from n_{iso}. So it is understandable that the various methods of determination of crystallinity may lead to some what different figures to the same polymers. Figure 8 shows the changes between crystallinity χ_c and draw ratio for viscose fibers, which decrease with increasing the draw ratios. So the chosen property for the structure properties such as refractive index, density, heat of fusion and modulus, the crystallinity may be the only parameter necessary for description.

Figures 9 and 10 show the relationship between the amorphous orientation function f_a, the crystalline orientation function f_c and draw ratio for viscose fibers. f_a decrease and f_c increase with increasing draw ratio.

Calculating the intrinsic crystalline and amorphous birefringence

Optical birefringence in uniaxially oriented polycrystalline polymers is given by Stein and Hermans[10,11] as follows

$$\Delta n = \Delta n_c^{\circ} + \Delta n_a^{\circ} \tag{14a}$$

Or rewritten to be

$$\Delta n = \chi\, \Delta n_c^{\circ} f_c + (1 - \chi)\Delta n_a^{\circ} f_a \tag{14b}$$

where $\Delta n_c^o = \chi\, \Delta n_c^{\circ} f_c$ and $\Delta n_a^o = (1 - \chi)\Delta n_a^{\circ} f_a$ are the intrinsic birefringence of the crystalline and amorphous phases, respectively; f_a and f_c are orientation factors and χ is the percentage crystallinity.

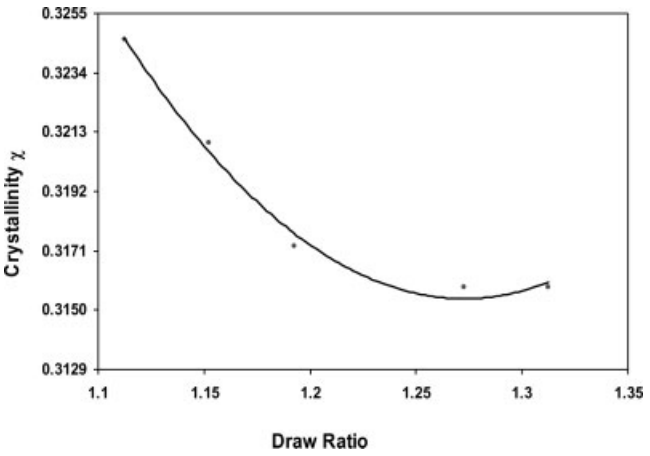

Figure 8 Relationship between crystallinity χ_c and draw ratio.

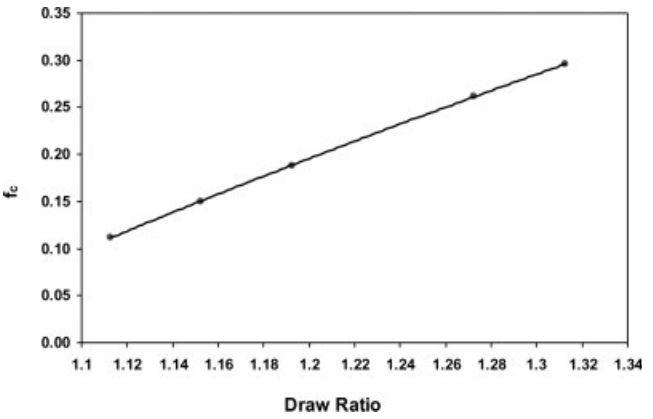

Figure 10 Relationship between the crystalline orientation function f_c and draw ratio for viscose fibers.

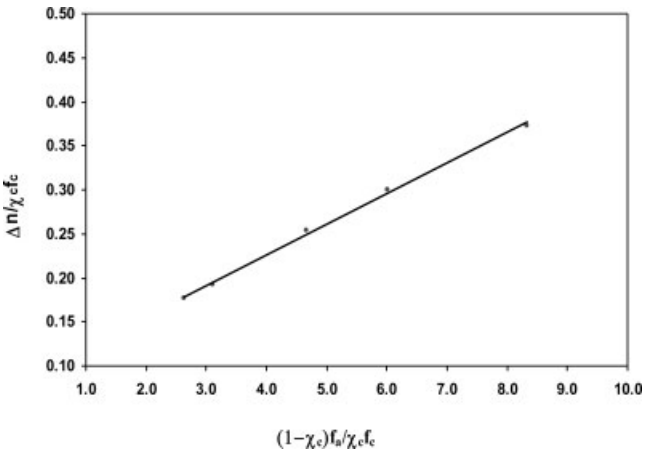

Figure 11 Relationship between $\frac{\Delta n}{\chi f_c}$ and $\left(\frac{1-\chi}{\chi}\right)\left(\frac{f_a}{f_c}\right)$, to determine Δn_c^o and Δn_a^o.

Rewriting equation (14-b) gives

$$\frac{\Delta n}{\chi f_c} = \Delta n_c^\circ + \Delta n_a^\circ \left(\frac{1-\chi}{\chi}\right)\left(\frac{f_a}{f_c}\right) \tag{15}$$

And a linear relationship is obtained between $\frac{\Delta n}{\chi f_c}$ such that $\left(\frac{1-\chi}{\chi}\right)\left(\frac{f_a}{f_c}\right)$. This relation can be used to determined Δn_c^o and Δn_a^o, where these intrinsic birefringence found to be 0.0877 and 0.0347, respectively from Figure 11.

Average optical orientation

It has to be stressed, however, that both crystalline and amorphous materials can exist in both oriented and unoriented states. So the average orientation F_{av} was calculated from the following equation[29]

$$F_{\text{av}} = 2\Delta n/\left(\Delta n_c^\circ + \Delta n_a^\circ\right) \tag{16}$$

where the denominator composed of the intrinsic birefringence of crystalline and the amorphous regions. The average orientation F_{av} increase with increasing draw ratio for viscose fibers as shown in Figure 12.

Equation of the mean square density fluctuation

For two phase structure consisting of amorphous and crystalline regions with densities ρ_a and ρ_c, respectively. The mean square density fluctuation $\langle \eta^2 \rangle$, can be calculated from the following equation.[30]

$$\langle \eta^2 \rangle = [\rho_c - \rho_a]^2 \chi[1-\chi] \tag{17}$$

Models for deformation of amorphous and partially ordered polymers

In the amorphous state, polymer chains are visualized as interpenetrating each other as they meander along what may be regarded as essentially random paths. Such interpenetrating paths create topographical entanglements that can only be eliminated by the repetition of chains along their paths to allow a chain end to slip through the entanglement. Two contrasting schemes have been proposed to account for the development of orientation during deformation. The first approximates the entangled polymer to a crosslinked rubber network where each chain between crosslinks can be represented by freely jointed rigid links and where the crosslinks deform in an affine manner along with the change of deforming body. Roe and Krigbaum[31] derived an expression for the distribution of segments at an angle θ with respect to the draw direction:

$$\omega(\cos\theta) = \frac{1}{2} + \frac{1}{4N_1}(3\cos^2\theta - 1)(D^2 - D^{-1}) \tag{18}$$

where N_1 is defined as the number of random links per chain. The second scheme considers the polymer only in terms of an aggregate of the segments that make up the chains. Before orientation, the segments will be randomly oriented at an angle θ with respect to the draw direction. After drawing the segments will be constrained at an angle β according to the pseudo-affine scheme, given by

$$\tan\beta = D^{-3/2}\tan\theta \tag{19}$$

The relation between tan θ and tan β with draw ratio are shown in Figure 13. Subsequent work[32] has demonstrated the applicability of these models to polymer deformation, respectively, above and below the T_g.

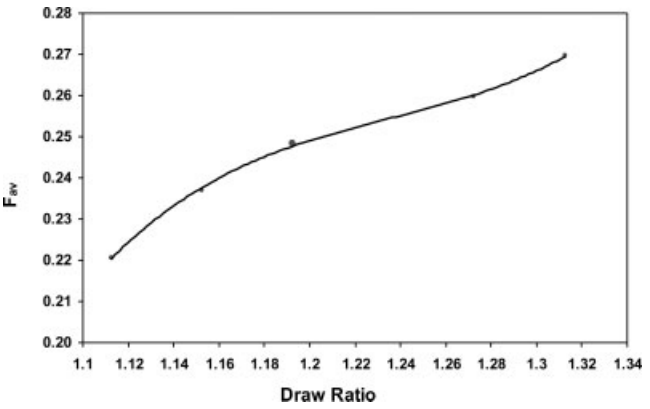

Figure 12 The average orientation F_{av}, at different draw ratio for viscose fibers.

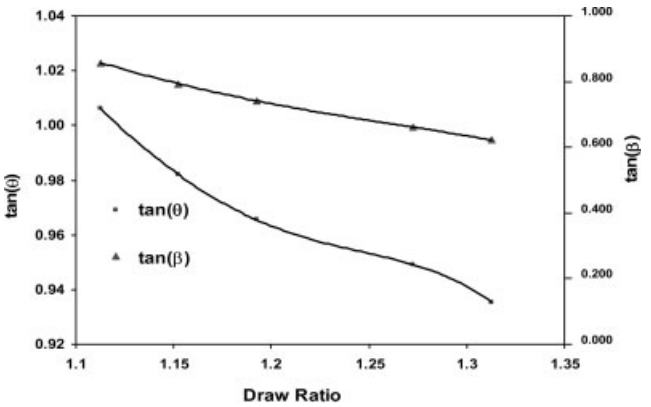

Figure 13 Relationship between tan θ and tan β.

For a random links, the orientation function $f_\Delta(\theta)$ as previously calculated[33] is given by

$$f_\Delta(\theta) = (D^2 - D^{-1})/5N_1 \tag{20}$$

from which N_1 can be obtained. The Kuhn-Treloar theory gives for $f_\Delta(\theta)$,

$$f_\Delta(\theta) = (2/5)N_c(D^2 - D^{-1}) \tag{21}$$

where N_c is the number of chains per unit volume and depends on the number of crystallinity in the polymer material.

The average work per chain W' for a collection of chains will depend on the distribution of chain-end distances, and is obtained by the following equation[34]

$$W' = \frac{3KT}{2}\left[\frac{1}{3}(D^2 - D^{-1}) + (D^{-1} - 1)\right] \tag{22}$$

where K is the Boltzman constant and T is the absolute temperature. Using Eq. (22) the average work per chain W' for viscose fiber was calculated and

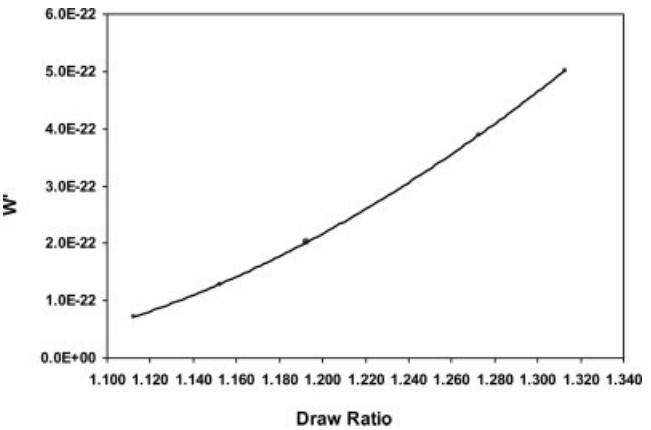

Figure 14 The average work per chain W' with draw ratio.

TABLE II
Values of Actual Draw Ratio, Isotropic Refractive Index n_{iso}, Density ρ, the Mean Square Density Fluctuation $\langle\eta^2\rangle$, the Number of Random Links Between the Network Points N_1, the Number of Chains Per Unit Volume N_c, and Distribution Function of Segment ω(cos θ)

D.R	n_{iso}	ρ	$\langle\eta^2\rangle$	N_1	N_c	ω(cos θ)
1.113	1.523	1.533	0.00405	0.2004	1.8113	0.7075
1.153	1.522	1.533	0.00403	0.2721	1.4310	0.7231
1.192	1.522	1.532	0.00401	0.3445	1.1841	0.7340
1.273	1.522	1.532	0.00400	0.4917	0.8672	0.7450
1.313	1.522	1.532	0.00400	0.5665	0.7806	0.7544

represented at different draw ratios as given in Figure 14. There was a gradual increase in the average work per chain with the draw ratio, which may be attribute to the rising of the work done on the fiber and the increasing the amount of the associated deformation.

The values of actual draw ratio, density ρ, the mean square density fluctuation $\langle\eta^2\rangle$, the number of random links between the network points N_1, the number of chains per unit volume N_c, and distribution function of segment ω(cos θ) are shown in Table II. An empirical formula was suggested to evaluate the relationship between draw ratio and Δn, $P_2(\theta)$, $f_2(\theta)$, f_c, δ_r, χ_c, and f_a as follows:

$$\ln[\Delta n P_2(\theta) f_2(\theta) f_c \delta_r/\chi_c f_a) = \mathrm{ADR} + B \tag{23}$$

where A and B are constants characterizing the proportionality in Eq. (23). The values of A and B were determined to be 10.906 and −20.594, respectively (Fig. 15).

So man-made fibers play an important role in the textile industry where most textiles are now mixed with synthetic and man-made yarns.

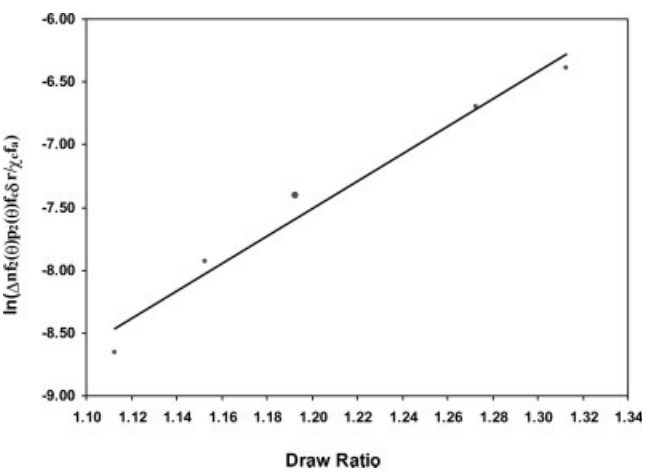

Figure 15 The relationship among ln [Δn $P_2(\theta)$ $f_2(\theta)$ f_c δ_r/ χ_c f_a) and draw ratio to determine the characterizing viscose material constants.

The degree of crystallinity and orientation of the fiber material and other structural parameters are correlated to the fiber end uses. Hence the optical parameter yield information about the orientations and the isotropic refractive index of the medium also gives information on crystallinity.

Deformation due to drawing process is the predominant means of producing new physical structures of polymeric fibers, which are commercially so important and are of much industrial interest. By means of the drawing process we produce an orientation in gaining greater insight at a micro-structure level when investigating mechanical properties.

As the mechanical strength can be further enhanced by orientation of the crystallites as induced by stretching. The orientation scheme, which describes the results obtained, assumes that viscose consists of an aggregate of transversely isotropic units whose symmetry axes rotate on drawing in the same manner as lines joining pairs of points in the bulk material, which deform at constant volume. So mechanical anisotropy for crystalline and glass polymers deformed by cold drawing enables the factor $P_4(\theta)$ as well as $P_2(\theta)$ to be calculated as a function of draw ratio.[24,33] The values obtained for $P_2(\theta)$ and $P_4(\theta)$ are particularly useful in predicting mechanical anisotropy for crystalline polymer deformed by cold drawing. The difference in their values with those of the optical orientation functions perhaps arises because the mechanical orientation functions depend only on the draw ratio. So uniaxial orientation is of the most importance in the production of man-made fibers. Only by stretching or drawing the spun filaments become dimensionally stable and lose their tendency to creep.

CONCLUSIONS

From the above discussion and considerations the following conclusions can be drawn:

1. The higher the orientation function, the more mutually parallel the molecules and the smaller the average angle formed by them with the fiber axis. These will be in agreement with the obtained result for the decrease in orientation angle with increasing draw ratios. The orientation functions given by the two techniques lead to an increase as the draw ratio increases. Where $f_\Delta(\theta)$, f_{mech}, f_c, $P_2(\theta)$, $P_4(\theta)$, and F_{av} increase but f_a decrease because of the decrease in crystallinity. The optical and mechanical techniques are suitable for the determination of molecular orientations parameters. The factor $P_4(\theta)$ is always comparatively small. So the mechanical method could be used for determining the orientation parameters with fair accuracy.
2. The obtained principal optical parameters are suitable for evaluating dielectric constant, the dielectric susceptibility, the surface reflectivity, and the crystallinity by using the isotropic refractive indices.
3. Both the shrinkage stress and the distribution function of segments increase as the draw ratio increases. Change in $\omega(\cos\theta)$ gives an indication for mass redistribution within the fiber chains and the three optical orientation function $f_\Delta(\theta)$, f_c, and f_a. The number N_1 of a random links between the network junction points per unit volume increases as the draw ratio increases.
4. As the crystallinity decreases with the increasing draw ratio, this behavior in the present result shows that deformation was accompanied by a reduction of crystallinity as shown in Figure 8.
5. Determination of the structural intrinsic birefringence per unit volume of a crystalline viscose fiber Δn_c^o and Δn_a^o for amorphous parts was found to be 0.0877 and 0.0347, respectively. Also Δn and the average work per chain W′ increase with increasing draw ratio.
6. Empirical formula was suggested to correlate some of the observed changes in the calculated parameters [Δn, $P_2(\theta)$, $f_2(\theta)$, f_c, δ_r, χ_c, and f_a] and the draw ratio of viscose fibers and found to be 10.906 and -20.594, respectively.
7. The Obtained principal optical parameters with the draw ratios could evaluate the constants A_2 and A_1 in Eq. (12). Where their ratios are approximately similar to C_2/C_1 for the Mooney-Rivilin equation, so the birefringence remains proportional to the stress.

References

1. Samuels, R. J. Structured Polymer Properties; Wiley: New York, 1974.
2. Barakat, N.; Hamza, A. A. Interferometry of Fibrous Materials; Hilger: UK, 1990.
3. Ward, I. M. Structure and Properties of Orientated Polymers Applied Science; London, 1975.
4. Stein, R. S. Polym Eng Sci 1965, 9, 320.
5. Fouda, I. M. J Polym Res 2002, 9, 37.
6. Fouda, I. M.; EL-Sharkawy, F. M. J Appl Polym Sci 2004, 91, 287.
7. Fouda, I. M.; Shabana, H. M. J Appl Polym Sci 1999, 72, 1185.
8. Fouda, I. M.; EL-Tonsy, M. M. Polym Plast Technol Eng 2006, 45, 223.
9. De Vries, H.; Bonnebat, C.; Beautemps, J. J Polym Sci Polym Symp 1977, 58, 109.
10. Stein, S. J Polym Sci 1959, 24, 709.
11. Hermans, P. H. Contributions to the Physics of Cellulose Fibres; North Holand: Amsterdom, 1949.
12. Treloar, L. R. G. Physics of Rubber Alasticity, 2nd ed.; Oxford University Press: London, 1958.

13. Ward, I. M. Proc Phys Soc London 1962, 80, 1176.
14. Ward, I. M. J Polym Sci Polym Symp 1977, 53, 9.
15. Hermans, P. H.; Platzek, P. Kollaid-Z 1939, 88, 67.
16. Gedde, U. F. W. Polymer Physics; Chapman & Hall: London, 1995.
17. Kratky, O. Kolloid-Z 1933, 64, 401.
18. Zbinden, R. Infrared Spectroscopy of High Polymers; Academic Press: New York, 1964.
19. Cunningham, A.; Davies, G. R.; Ward, I. M. Polymer 1976, 15, 743.
20. Gaylord, R. J. Polym Lett 1975, 13, 337.
21. Krigbaum W. R.; Roe, R. I. J Polym Sci 1964, 4, 4391.
22. Kitamara, R.; Dong, H.; Tsup, W. Int Symp Macromol Chem Prepr 1966, 8, 98.
23. Vank Revelen, D. W. Properties of Polymers; Elsevier: New York, 1976. p 237.
24. Hemsley, D. A. Applied Polymer Light Microscopy; Elsevier: London, 1989.
25. Jenkins, A. D. Polymer Science Handbook, Vol. l; North Holland: Amsterdam, 1972 (Contained the ref.: (i) Mooney, M. J Appl Phys 1946, 11, 582; (ii) Mooney, M. J Appl Phys 1948, 19, 434; (iii) Rivlin, R S. Trans R Soc London 1948, A241, 379).
26. Fouda, I. M. J Appl Polym Sci 1999, 73, 819.
27. Fouda, I. M.; Shabana, H. M. Eur Polym J 2000, 36, 823.
28. Monobe, S.; Kamide, R. J Text Plach Soc Jpn 1981, 34, 98.
29. Wesolowska, E.; LeWaskiewicz, W. J Polym Sci Phys Ed 1975, 13, 835.
30. Ficher, E. W.; Fakirov, S. J Mater Sci 1975, 11, 955.
31. Roe, R. J.; Krigbaum, W. R. J Appl Phys 1964, 35, 2215.
32. Ward, I. M. Br J Appl Phys 1967, 18, 1165.
33. Perena, J. M.; Duckett, R. A.; Ward, I. M. J Appl Polym Sci 1980, 25, 1381.
34. Williams, D. J. Polymer Science and Engineering; Prentice-Hall: England Wood Cliffs, NJ, 1971.